Environmental Pollution 288 (2021) 117779

Contents lists available at ScienceDirect

Environmental Pollution

journal homepage: www.elsevier.com/locate/envpol

Transport and dilution of fluvial antibiotic in the Upper Gulf of Thailand☆

Aobo Wang [a], Xinyu Guo [b,*], Akihiko Morimoto [b], Kana Maetani [a], Rumi Tanoue [b], Siraporn Tong-U-Dom [c], Anukul Buranaprattheprat [c]

[a] Graduate School of Science and Engineering, Ehime University, Matsuyama, Japan
[b] Center for Marine Environmental Studies (CMES), Ehime University, Japan
[c] Department of Aquatic Science, Faculty of Science, Burapha University, Thailand

ARTICLE INFO

Keywords:
Sulfamethoxazole
Dilution ratio
Mass balance
Fluvial pollutant
Prediction function

ABSTRACT

A three-dimensional hydrodynamic-antibiotic model is developed to investigate the transport and dilution of sulfamethoxazole (SMX) in the Upper Gulf of Thailand (UGoT). The simulation produced a spatially averaged annual mean SMX concentration of 0.58 μg m^{-3}, which varied slightly between seasons assuming a temporally constant river SMX loading observed in August. In contrast, the horizontal distribution of SMX concentrations strongly varied with season because of the changing residual currents. In addition, SMX is diluted to concentrations lower than 10% of those in river waters a short distance offshore of the estuaries. To better understand this behavior, we examined the relationship between salinity and SMX concentrations in the UGoT. The annual budget demonstrates that 98% of SMX in the UGoT is removed by natural decomposition. As the concentrations of fluvial pollutants in the UGoT depend on their river loading and decomposition rates, functions were derived to predict pollutant concentrations and flushing times based on the river input flux and half-life.

1. Introduction

Antibiotics are emerging organic pollutants widely used in human therapy, veterinarians, agriculture, and aquaculture because of their medicinal properties, growth-promoting properties, and breeding applications (Tamtam et al., 2008; Jiang et al., 2011; Kafaei et al., 2018). The increasing use of antibiotics and the resulting accumulation of antibiotic residues in the environment present serious problems. This includes harm to biological communities by destroying the ecological balance and the emergence of antibiotic resistance genes (Isidori et al., 2005; Martínez, 2008; Kummerer, 2009; Zhang et al., 2018).

The ocean is an important sink for many terrestrial pollutants (Sabourin et al., 2012; Zhang et al., 2013b; Ko et al., 2014; Downs et al., 2016; Ju et al., 2016). Some studies have indicated that the annual global consumption of antibiotics is 100,000 to 200,000 tons, which is linked to antibiotic pollution in a variety of environmental media, including ocean water (Zuccato et al., 2010; Kafaei et al., 2018). Indeed, several kinds of antibiotics, including sulfonamides, macrolides, fluoroquinolone, trimethoprim, cephalexin, amoxicillin, carbamazepine, and orphenadrine, have been detected at concentrations of μg L^{-1} in seawater including in the Bohai Sea, South China Sea, Baltic Sea, and the coastal areas of Iran (Zhang et al., 2013a; Björlenius et al., 2018; Kafaei et al., 2018; Zhang et al., 2018).

Previous studies have shown that large amounts of antibiotics are discharged into coastal waters from rivers, after which they are transported by ocean currents and ultimately decomposed by organisms and light (Jia et al., 2011; Li et al., 2011; Zou et al., 2011). Antibiotics from rivers can be diluted in seawater, and their concentrations are inversely proportional to the salinity, showing high dispersion (Du et al., 2017). The partitioning of antibiotics to aerosols is weak because they are mostly polar or ionic, indicating that atmospheric deposition of antibiotics is insignificant (Zhang et al., 2013a).

The observation of antibiotics in seawater helps determine pollution levels and evaluate their environmental effects and fate (Zhang et al., 2015). However, the field data on antibiotics are usually not continuous in time and space due to natural, economic, and practical constraints (Zhang et al., 2015; Zhu et al., 2019). For example, a bad weather usually does not allow a survey over sea. Meanwhile, the field observation cannot quantify the flux of each process contributing to the variation of concentration of antibiotics.

Ocean models are useful tools to solve the problems mentioned above by simulating the continuously spatial and temporal variations of

☆ This paper has been recommended for acceptance by Maria Cristina Fossi.

* Corresponding author.
E-mail address: guoxinyu@sci.ehime-u.ac.jp (X. Guo).

https://doi.org/10.1016/j.envpol.2021.117779
Received 22 October 2020; Received in revised form 1 July 2021; Accepted 10 July 2021
Available online 13 July 2021

pollutants and calculating the pollutant flux of each biogeochemical processes contributing to these variations. For example, ocean models for suspended sediment, nutrients, and persistent organic pollutants (POPs) have been used to investigate their physical and biogeochemical processes (Bian et al., 2013; Wang et al., 2019a; Wang et al., 2019b; Zhang et al., 2019). However, to date, few simulations have been performed for antibiotics in seawater. One recent study found that the concentrations of antibiotics in the Seto Inland Sea decreased with a reduction in half-life, deriving a power function relationship between them (Zhu et al., 2019).

The Upper Gulf of Thailand (UGoT) is a semi-closed shallow sea located in the northern area of the Gulf of Thailand, which is located in the tropical area on the western side of the South China Sea and is surrounded by Thailand, Vietnam, Cambodia, and Malaysia (Fig. 1) (Boonyatumanond et al., 2007; Yu et al., 2018). The UGoT is affected by wet southwesterly monsoon conditions from May to September and dry northeasterly monsoon conditions from November to January (Yu et al., 2018). The area is bordered by several large cities in Thailand, including Bangkok, and is affected by significant human activity (Burnett et al., 2007). There are four rivers around the UGoT, namely the Bangpakong, Chaopraya, Thachin, and Maeklong Rivers, which flow through several cities and deliver large amounts of urban discharge to the UGoT (Yu et al., 2018). The combined annual mean river discharge of these four rivers is 960 $m^3\ s^{-1}$. Among the four rivers, the Chaopraya River has a maximum annual mean runoff of 365 $m^3\ s^{-1}$ (Buranapratheprat et al., 2008; Yu et al., 2018).

Sulfamethoxazole (SMX), a widely used sulfonamide, is generally used to treat urinary infections in humans as well as in veterinary, aquaculture, and livestock breeding to treat disease and promote growth (Drillia et al., 2005; Xu et al., 2011). SMX is widely detected in groundwater, rivers, and seawater worldwide (Watkinson et al., 2009; Tewari et al., 2013; Zhang et al., 2013a; Du et al., 2017; Chen et al., 2018; Li et al., 2018) and it is integrated into biogeochemical cycle via hydrolysis, biodegradation, and adsorption to sediment (Li, 2014). The half-life of SMX is reported to be 14.9 days in the sediment-seawater system (Xu et al., 2009) but 3, 9, 16, 49, 85, and >100 days in other experimental conditions, as shown in Table S1 (Benotti and Brownawell, 2009; Baumgarten et al., 2011). Among those values, we chose 14.9 days (bolded in Table S1) as a default half-life of SMX in the UGoT because experiment conditions used by Xu et al. (2009) were similar to the marine environment in the UGoT (details of the experiment conditions are shown in Appendix A of the supplementary material).

Previous work indicates that the canals and river systems of economically productive cities around the UGoT are threatened by antibiotic residues of various origins (Tewari et al., 2013; Mrozik et al., 2019). However, there is little information regarding the occurrence and concentrations of antibiotics in seawater in the UGoT. In addition, river discharge and ocean currents in the UGoT show strong seasonality due to the monsoon system and rainfall, which can affect pollutant concentrations. Therefore, there is a need to determine the extent and degree of antibiotic pollution in the UGoT, and to examine the effects of environmental factors on spatial and temporal variations of pollution.

Here, SMX was chosen as the target pollutant, having high ecological risk in some coastal waters (Zhang et al., 2013a, 2013b; Du et al., 2017). We use a three-dimensional (3D) model to simulate the temporal and spatial variations of SMX in the UGoT, to calculate its dilution ratio and budget in seawater, and to examine the relationship between salinity and SMX concentrations. Furthermore, we develop a prediction function for the concentration of pollutant in the UGoT based on its half-life and river input load.

2. Field sampling and model description

2.1. Field sampling and SMX analysis

River and seawater surface water samples were collected in August 2019 including 12 samples from the UGoT and four samples from the Bangpakong River, Chaopraya River, Thachin River, and Maeklong River estuaries (Fig. 1b; Table S2). The samples in the sea were collected on the ship deck while those in estuaries were collected along the shore side. The samples of river water and seawater were all collected for the surface water using a stainless steel bucket. After three times of washing the amber polypropylene bottles using the collected surface water, the surface water was saved in the bottles. After adding 1.0 $g\ L^{-1}$ ascorbic

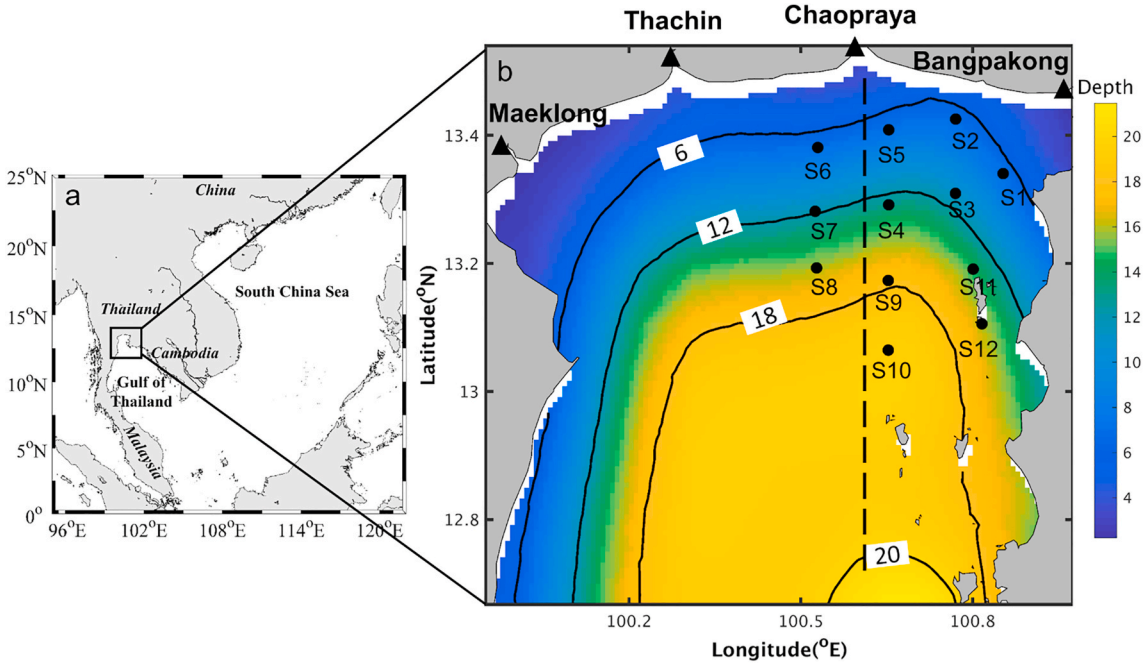

Fig. 1. (a) Location of the Upper Gulf of Thailand; (b) Model domain and bathymetry (color shading for depth and contours are in meters). Black triangles are the estuaries of the Bangpokong, Chaopraya, Thachin, and Maeklong Rivers. Black dots represent the SMX water sampling stations sampled in August 2019. The dashed line indicates the section shown in Fig. S2. (For interpretation of the references to color in this figure legend, the reader is referred to the Web version of this article.)

acid to it, we stored the amber polypropylene bottles in darkness at −20 °C prior to analysis. The details of SMX analysis are shown in Appendix B.

2.2. Model description

A 3D hydrodynamic-antibiotic model was developed to simulate the transport and dilution of SMX from rivers in the UGoT. The model includes two parts, a hydrodynamic module and an antibiotic module. Using this model, we simulated the distribution of SMX from different rivers and examined the effects of the half-life on their spatial and temporal variations in the UGoT.

2.3. Hydrodynamic module

The hydrodynamic module is the same as that used to study the seasonal variations of low-salinity water in the UGoT (Yu et al., 2018), based on the Princeton Ocean Model (Mellor et al., 2002). The model domain extended from 99.9500 °E to 100.9750 °E and from 12.6666 °N to 13.5083 °N (Fig. 1b) with horizontal resolution of ~1 km and a vertical resolution of 21 sigma layers (0.000, −0.002, −0.004, −0.010, −0.020, −0.040, −0.060, −0.080, −0.100, −0.120, −0.140, −0.170, −0.200, −0.300, −0.400, −0.500, −0.650, −0.800, −0.900, −0.950, −1.000).

The forcing data of the hydrodynamic model include monthly heat flux, wind stress, river discharge, water temperature and salinity at the open boundary, and tide height at the open boundary datasets obtained from Buranapratheprat et al. (2008, 2009). Given the small size of the UGoT (approximately 100 km × 100 km, Yu et al., 2018), the surface forcing data were assumed to be horizontally homogeneous in the model. For the tides, four tide constituents (M_2 , S_2 , K_1, and O_1) were added to the elevation at the open boundary (Yu et al., 2018). These forcing conditions are for a simulation of the climatological state in the UGoT.

2.4. Antibiotic module

SMX was considered in the model in its dissolved state, with concentrations expressed as C_1, C_2, C_3, C_4, for the Bangpakong River, Chaopraya River, Thachin River, and Maeklong River contributions, respectively. As well as advection and diffusion, SMX was assumed to decompose in the seawater (Fig. S1). The concentration of dissolved SMX was calculated using the following equation.

$$\frac{\partial C}{\partial t}+u\frac{\partial C}{\partial x}+\mathrm{v}\frac{\partial C}{\partial y}+w\frac{\partial C}{\partial z}=\frac{\partial}{\partial z}\left(K_h\frac{\partial C}{\partial z}\right)+D(C)+S(C)+Dec(C) \quad (1)$$

In the equation, C (μg m^{-3}) is the concentration of SMX in seawater driven by one of the four rivers (C_1, C_2, C_3, C_4); t is time (s); x, y, and z are the zonal, meridional, and vertical coordinates (m); u, v, and w are the velocity components in the x, y, and z directions, respectively (m s^{-1}); K_h is the vertical eddy diffusion coefficient (m^2 s^{-1}); $D(C)$ is the horizontal diffusion term; $S(C)$ is the source term; and $Dec(C)$ is the decomposition term. Some research reported back-transformation of SMX from degradation products (Nödler et al., 2012; Bonvin et al., 2013). However, we did not include this process in the model because its small flux. A detailed explanation is given in Appendix C. Equation (1) is calculated in two steps: an explicit scheme for horizontal and vertical advection, horizontal diffusion, and the source and decomposition terms, and an implicit scheme for vertical diffusion (Mellor et al., 2002).

We assumed that SMX in the UGoT could only be sourced from the four rivers. Therefore, $S(C)$ (μg m^{-3} s^{-1}) is equaled to the SMX loads of the rivers at the grid points corresponding to the estuaries but was set to zero at the other grid points. The SMX load from each river was calculated as follows:

$$F_{river}(C)=Q\times C_r \quad (2)$$

where $F_{river}(C)$ (μg s^{-1}) is the river input load, Q (m^3 s^{-1}) is the river runoff, and C_r (μg m^{-3}) is the concentration of SMX in the river water. When $F_{river}(C)$ is to the grid point of the estuary, it is diluted by the seawater corresponding to that grid point, that is, $S(C) = (F_{river}(C) + C_0 \times V_0)/(Q + V_0)$, where C_0 is the SMX concentration at the estuary grid point and V_0 is the volume of seawater at the grid point.

The SMX decomposition term in Eq. (1) is described as follows:

$$Dec(C)=-\ln 2\times\alpha^{-1}\times C \quad (3)$$

where $Dec(C)$ (μg m^{-3} s^{-1}) is the SMX decomposition flux and α (s) is the SMX half-life (Table S1). We assumed a SMX half-life 14.9 days, as this was experimentally derived in seawater (Xu et al., 2009). Eqs. (1)–(3) can be applied to SMX from each river (C_1, C_2, C_3, and C_4), referred to as Cases 1 to 4. As Eq. (1) represents a linear system, the total SMX concentrations in the sea were determined as the sum of C_1, C_2, C_3, and C_4.

The initial concentration of SMX in the model domain was set to 0 in the four cases. During the calculation, the SMX concentration gradient across the open boundary was set to zero. The SMX concentrations in the river waters in August 2019 are shown in Table S3, and mean river discharge for August 2019 was used to obtain the SMX flux from each river to the UGoT. Based on the assumption that the usage of SMX in the cities around the UGoT varies little throughout a year, the SMX flux from each river was held at the August 2019 level throughout the calculation. To avoid the influence of the initial conditions, we run the model for a three-year period, using the results for the third year in our analysis.

3. Results

3.1. Seasonal variations and spatial distribution of SMX in the UGoT

SMX transport from each of the four study rivers was simulated by the model. As shown in Fig. 2, the calculated concentrations in the second and third years of the simulation are almost the same, indicating that the calculation reached a stationary state after the second year. In the following analysis, we use the results in the third year to examine the temporal and spatial variations in the SMX in the UGoT. The notable small oscillations in Fig. 2 have a period of approximately 15 days, reflecting the cycle of SMX exchange with the open sea driven by spring and neap tides.

Although we used a temporally constant river input flux of SMX, the concentrations of it varied in the UGoT across the year (Fig. 2). A maximum concentration of 0.68 μg m^{-3} occurs in February and a minimum of 0.45 μg m^{-3} occurs in November (Fig. 2). Such seasonal variations are attributed to a weak residual current in February, which is not favorable for SMX transport out from the UGoT. Among the four rivers, the concentrations of SMX delivered from the Chaopraya River are highest, having a dominant control on the seasonal variations in the UGoT, which is due to the highest input flux of SMX from Chaopraya River (Table S3).

February, August, October, and November were chosen to examine the spatial distributions of monthly averaged SMX concentrations (Fig. 3). These months were selected as the northeastward wind and southwestward wind prevailed in August and November, respectively, and the transition of wind occurred in October. Furthermore, the highest mean concentration of SMX occurred in February (Fig. 2).

As shown in Fig. 3, the model results for August are generally consistent with the spatial variation of surface SMX concentrations based on the field data, being high in nearshore areas and low in offshore areas. The concentrations of SMX at stations S1 S3–S5, S9, and S11–S12 match well with the field data; however, the concentrations at stations S7 and S10 are higher than the field data, while those at stations S2, S6 and S8 are lower. Another difference is the patches of high or low concentrations in the field data but only a smoothly spatial change in the SMX concentrations of model results. This likely reflects the field data

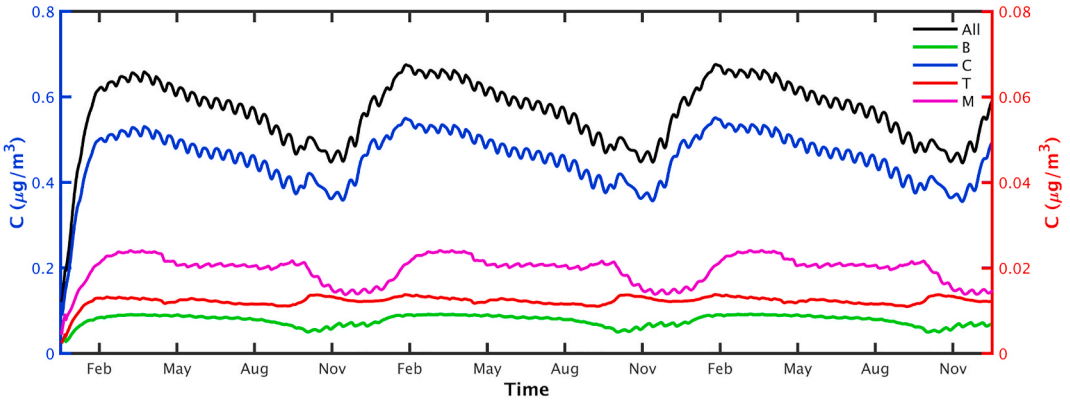

Fig. 2. Time series of mean SMX concentrations over the entire model domain during the three-year calculation period. 'All' represents SMX from all four rivers, and 'B', 'C', 'T', 'M' represent SMX from the Bangpakong, Chaopraya, Thachin, and Maeklong Rivers, respectively. The black, blue, and green lines refer to the left-hand y-axis and the magenta and red lines refer to the right-hand y-axis. (For interpretation of the references to color in this figure legend, the reader is referred to the Web version of this article.)

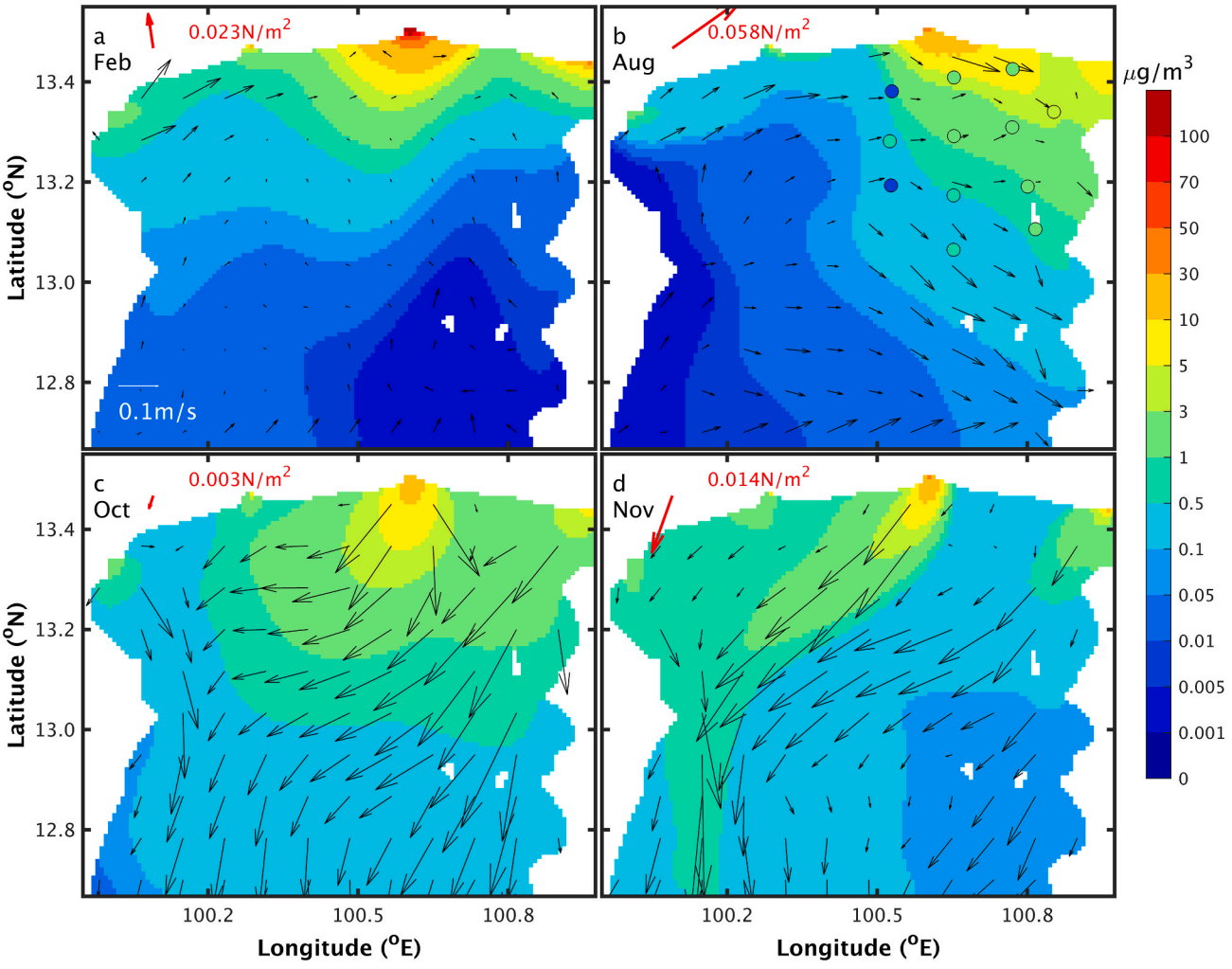

Fig. 3. Horizontal distribution of monthly averaged surface SMX concentrations and residual currents in (a) February, (b) August, (c) October, and (d) November. The black arrows represent residual currents and the red arrows represent wind stress. The filled circles in (b) are the SMX field data in August 2019. The color scale is the same for the model results and field data. The "surface layer" in the model occupies 0.2% of the water column depth that is the thickness of first sigma coordinate. The "surface" for field data means the sampling of surface water that is around the layer of 0–0.1 m. Because of the presence of surface mixed layer that is at an order of meters even in summer, the "surface" for model and field sampling have not essentially difference for the SMX concentration. (For interpretation of the references to color in this figure legend, the reader is referred to the Web version of this article.)

only capturing a snapshot of time, while the model results are averaged by month.

The horizontal distribution of SMX concentrations is strongly affected by residual currents. In February, the residual current is generally weak, when SMX accumulates around the estuary regions and decreases in concentration from north to south, yielding the steepest gradient among the four studied months (Fig. 3). In August, SMX concentrations decrease from northeast to southwest, which is consistent with the eastward and southeastward residual currents. The SMX concentrations in October decrease from the coastal area to the open boundary due to the southward and southwestward currents. In November, concentrations are higher in the northwest than in the southeast, which reflects the westward and southwestward currents.

Residual currents in the UGoT are affected by river runoff, wind, and the Coriolis force (Yu et al., 2018). The slow currents in February are induced by weak winds and small amounts of river runoff. Although the UGoT is not positioned at a very high latitude, the influence of the Coriolis force on residual currents can still be observed. For example, the northeastward monsoon causes residual currents to flow eastward and southeastward in August. In October, wind speed is lower and the southwestward residual currents are mainly affected by diluted river water and the Coriolis force. The residual currents in November are mainly southwestward, likely resulting from the southward wind and the Coriolis force.

A section across the UGoT (Fig. 1) was chosen to examine the vertical distribution of SMX in more detail. As shown in Fig. S2, simulated SMX concentrations vary vertically in the coastal areas near the estuary while being almost homogeneous offshore. As low-salinity water flows into the sea from the estuary along with the pollutant, higher SMX concentrations occur at the sea surface. Subsequently, the surface layer is mixed vertically from the estuary area to offshore area by winds and tidal currents. Consequently, the model simulates relatively homogenous vertical SMX concentrations in the offshore area.

3.2. Dilution of SMX from different rivers

The distribution of SMX in the UGoT from each river is affected by its concentration in river water, the river runoff, the location of estuaries, and the residual currents in the UGoT (Fig. 4). The concentration of SMX decreases from the estuary of the Bangpakong River to the west and south of the UGoT. As shown in Fig. 4a1–a4, the area with SMX concentrations higher than 0.001 μg m^{-3} is smaller in February and August

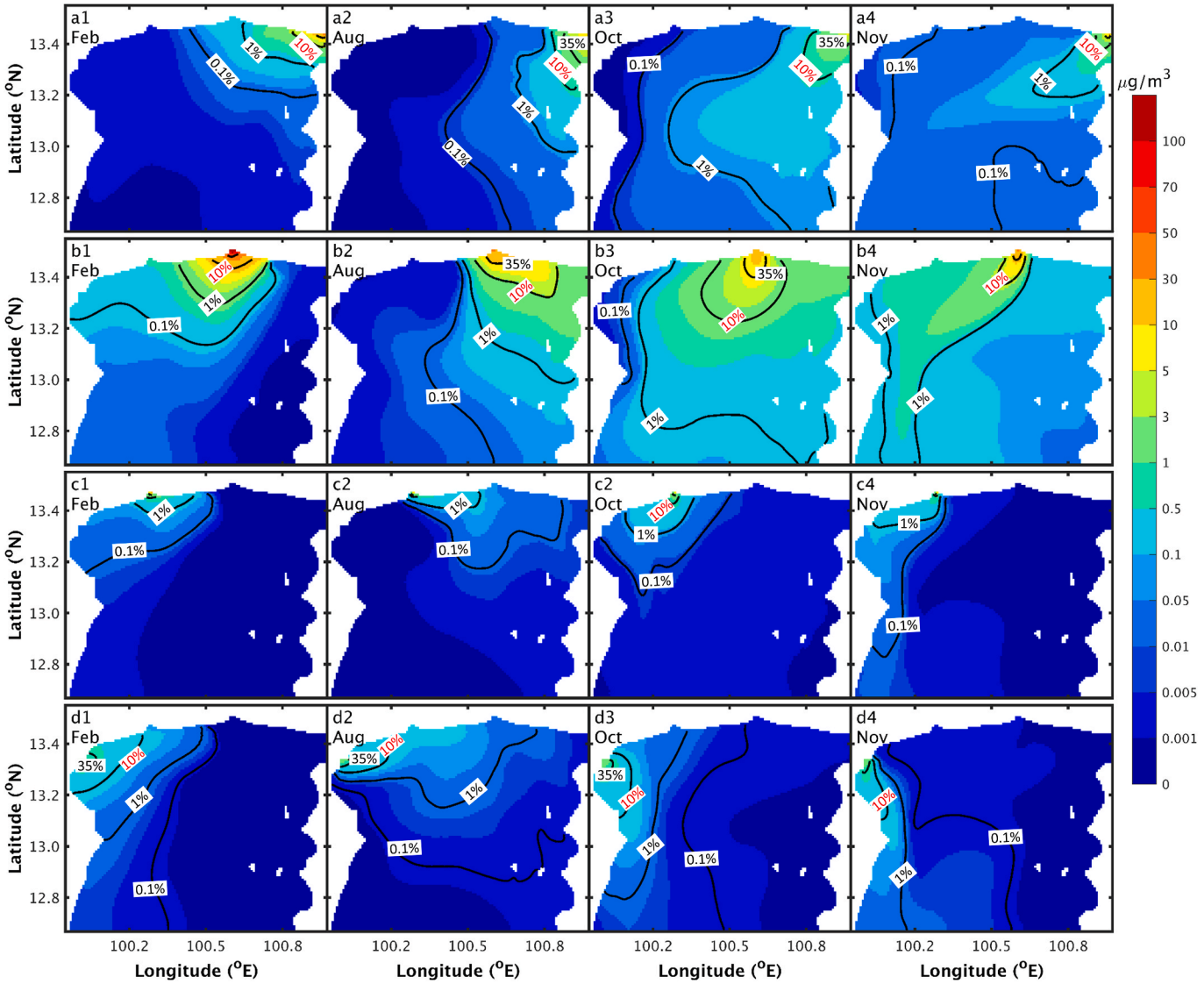

Fig. 4. Horizontal distribution of monthly averaged surface concentrations and dilution ratios of SMX from the (a1–a4) Bangpakong, (b1–b4) Chaopraya, (c1–c4) Thachin, and (d1–d4) Maeklong Rivers. Color shading represents SMX concentrations and contours represent dilution ratios. (For interpretation of the references to color in this figure legend, the reader is referred to the Web version of this article.)

than in October and November, which is likely caused by the slow, eastward residual currents and southwestward residual currents, respectively. SMX concentrations decrease from the estuary of the Chaopraya River to the south in February, being low in the southeast due to the input of water from the open sea. SMX from the Chaopraya River is transported to the southeast in August and the southwest in October and November. The transport characteristics of SMX from the Thachin River are similar to those of the Chaopraya River. For the Maeklong River, SMX concentrations decrease from its estuary to the south and east areas of the UGoT. The area with an SMX concentration higher than 0.001 $\mu g\ m^{-3}$ is smaller in February than in other studied months (Fig. 4d1–d4).

To investigate the general dilution characteristics of SMX from each river, dilution ratios were calculated as $D_r = \frac{C}{C_r} \times 100\%$, where D_r is the dilution ratio, C ($\mu g\ m^{-3}$) is the monthly averaged concentration of SMX in seawater originating from a river, and C_r ($\mu g\ m^{-3}$) and is the monthly averaged concentration of SMX in the river water. Unlike the SMX concentration simulated for seawater, the dilution ratios are independent of the river water concentration.

The SMX dilution ratios from all four rivers are plotted in Fig. 4, which extend in the same direction as the SMX concentration as previously described. The extended range of the dilution ratios is affected by the residual currents, as controlled by wind stress and river runoff. The 10% dilution ratios of SMX for the four rivers occur at different distances from their respective estuaries; based on the outermost points on the 10% contour from the estuaries, these distances vary between 7 and 25 km for the Bangpakong River in different months, 9–32 km for the Chaopraya River, and 23–30 km for the Maeklong River. In comparison, SMX concentrations become less than 10% of those in the Thachin River over a very short distance from the estuary.Where field data of river concentration are available, dilution ratios can be used to deduce the SMX concentrations in seawater using Eq. (4):

$$C = \sum_{n=1}^{4} C_{rn} \times D_{rn} \tag{4}$$

where C is the SMX concentration in seawater, n is an index for a river, C_{rn} is the SMX concentration in the nth river, and D_{rn} is the SMX dilution ratio from the nth river, whose value at every grid point is given in Fig. 4.

3.3. Mass balance of SMX in the UGoT

The SMX in the model domain derives from rivers and undergoes decomposition in seawater and transport by ocean currents. To study the behaviors of SMX quantitatively, the fluxes related to these processes were calculated as 15-day mean values to filter out tidally driven oscillations (Fig. 5). SMX flux from the rivers is assumed constant in the model while decomposition is dynamic. The poor water exchange with the open sea causes the accumulation of SMX in the UGoT from February to September, which leads to the highest decomposition flux occurring in October (Fig. 5). The poor exchange with the open sea is also indicated by SMX flux through the open boundary, which is close to 0 from February to September (Fig. 5) when the northeastward or northward monsoon drives an eastward or northeastward current. From October to the following January, SMX is removed from the UGoT through the open boundary in association with the southward currents.

The annual SMX budget was evaluated by integrating the different fluxes in Fig. 5 based on $\int_1^{365} \iiint F(x,y,z)dxdydzdt$, where F $\left(\text{kg m}^{-3}\ \text{day}^{-1}\right)$ is the flux of each process; dx, dy, and dz are unit distance (m) in three directions; and dt is the unit time interval (day). The volume integral was for the entire UGoT and the time integral was one year. As shown in Table 1, the Chaopraya River is the dominant source of SMX (82%) in the UGoT. Approximately 98% of the SMX from rivers is removed by decomposition, while only 2% is removed via horizontal advection through the open boundary. The annually averaged SMX mass in the UGoT is 37.5 kg.

Subsequently, the flushing time was calculated as the ratio of SMX mass inside the UGoT to the flux of SMX removed from the system (Monsen et al., 2002), as follows:

$$t_r = \frac{M}{F_{ob} + F_{cwd}} \tag{5}$$

where t_r is the flushing time, M is the mass of SMX, and F_{ob} and F_{cwd} are the SMX fluxes through the open boundary and via decomposition, respectively. Based on this, a flushing time of SMX in the UGoT is approximately 21 days. Based on the same method, the flushing time of

Table 1
Annually averaged SMX mass balance in the model. 'B', 'C', 'T', and 'M' indicate the Bangpakong, Chaopraya, Thachin, and Maeklong Rivers, respectively.

River input (kg yr^{-1})				Open boundary (kg yr^{-1})	Decomposition (kg yr^{-1})	Annual mean of SMX mass (kg)
B	C	T	M			
83.2	535.0	11.8	21.3	9.9	639.8	37.5

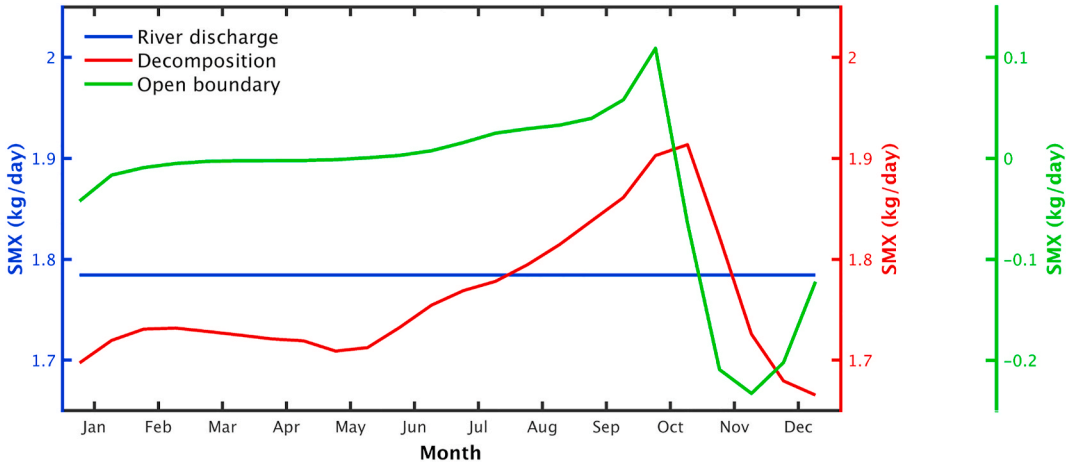

Fig. 5. Time-series of SMX fluxes from rivers (blue line), through the open boundary (green line), and via decomposition (red line). The lines represent mean values over 15 days. A negative flux through the open boundary indicates a loss of SMX, while a positive flux means a gain. Line colors in the plot indicate the corresponding axes. (For interpretation of the references to color in this figure legend, the reader is referred to the Web version of this article.)

diluted water from the rivers is much longer at approximately 169 days.

4. Discussion

4.1. Relationship between salinity and SMX concentrations

The relationships between salinity and contaminant concentrations are often used in provenance studies in seawater. In general, the concentration of a pollutant in the sea shows an inverse linear relationship with salinity if the pollutant has a sole origin from rivers. However, as shown in Fig. 6, the modeled relationship can be represented by four different lines denoting variable SMX concentrations for the same salinity conditions in the UGoT.

The pollutant concentration and salinity at one point in the UGoT can be represented by Eq. (4) (see Section 3.2) and Eq. (6), as follows:

$$S = S_0\left(1 - \sum_{n=1}^{4} a_n\right) \tag{6}$$

where S is the salinity of the seawater, n is the index for a river, S_0 is the salinity in the open sea, and a_n is the proportion of nth river water in the seawater.

If there is only one river flowing into the UGoT, Eqs. (4) and (6) can be simplified to Eqs. (7) and (8):

$$C = C_{r_1} \times D_{r_1} \tag{7}$$

$$S = S_0(1 - a_1) \tag{8}$$

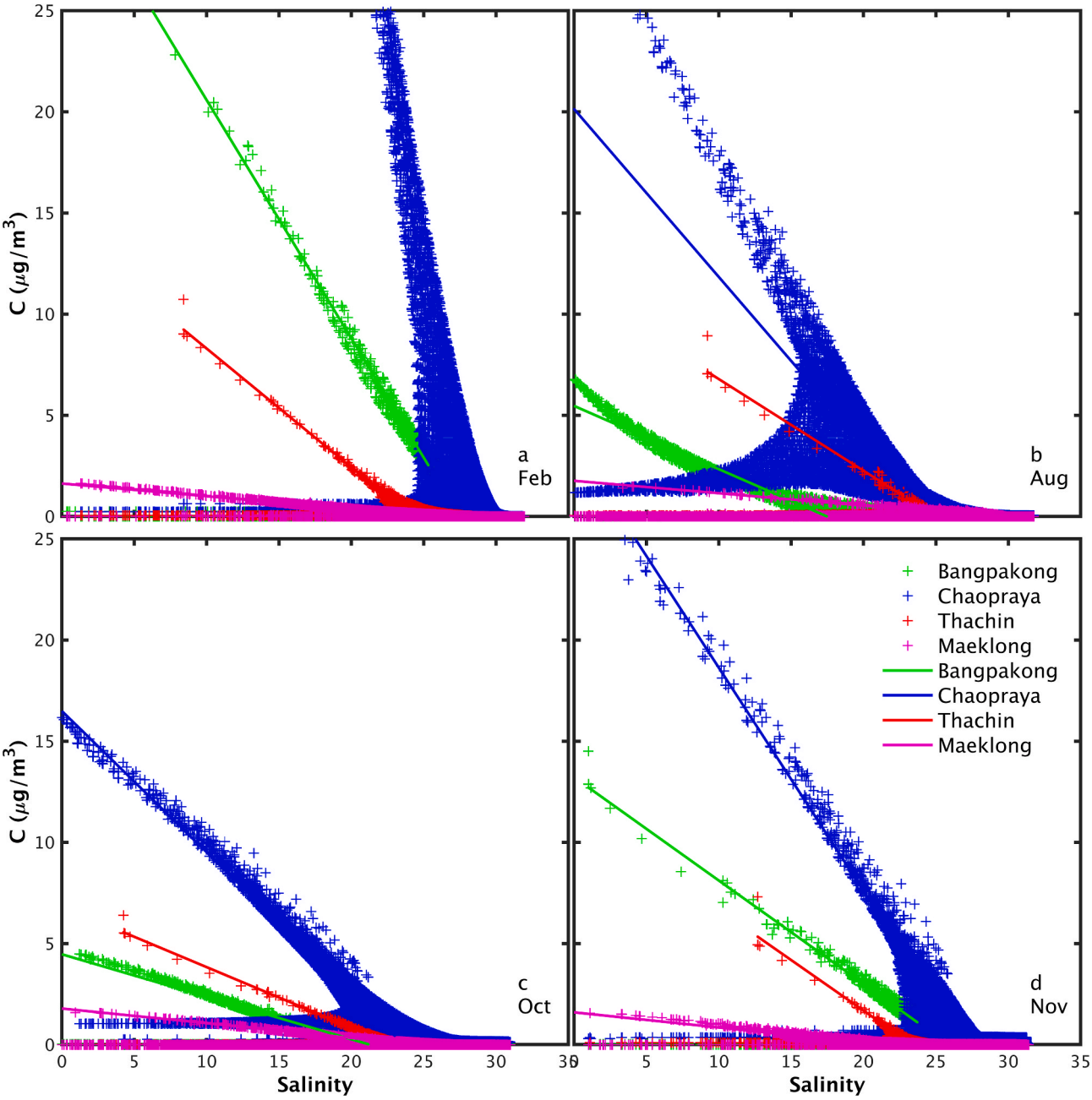

Fig. 6. Relationships between monthly averaged salinity and SMX concentrations of the whole water column in the UGoT. The plus signs with different colors represent model results driven by each corresponding river; the regression lines are deduced in the area with the dilution ratio larger than 10%. (For interpretation of the references to color in this figure legend, the reader is referred to the Web version of this article.)

where C_{r_1} is the concentration of pollutant in the target river, D_{r_1} is the dilution ratio of pollutant from the river, and a_1 is the proportion of the river water in seawater. D_{r_1} equals a_1 at every point when the pollutant is persistent, and its transport in the sea is the same as that for the dilution water. As a result, it is deduced from Eqs. (7) and (8) that the concentration of a pollutant in seawater (C) is linearly related to the salinity (S) with the slope and intercept $-\frac{C_{r_1}}{S_0}$ and C_{r_1}, respectively. If the pollutant from a river is decomposable, D_{r_1} is different from a_1 for the dilution water. Moreover, the relationship between C and S at different points in the sea is affected by D_{r_1} and a_1.

Actually, there are four rivers around the UGoT, and the persistence of pollutants from rivers is not the only requirement for maintaining a linear relationship between the pollutant concentrations and salinity; the concentration of pollutants in the four study rivers must also be the same. When these two requirements are true, D_{rn} in Eq. (4) is equal to a_n in Eq. (6), and C_{rn} in Eq. (4) is a constant. Under such conditions, the concentration of pollutant (C) driven by the four rivers is linearly related to salinity (S) in the UGoT. Otherwise, the relationship between C and S is affected by a_n, D_{rn}, and C_{rn}.

As previously noted, the concentrations of SMX in the waters of the four rivers are different and SMX is also decomposable in seawater. Thus, the SMX concentrations are not linearly related to the salinity in the UGoT. A linear relationship should exist, however, in those areas controlled by a single river, where SMX can be considered as a passive tracer given its short residency time after leaving the estuaries and the low levels of dilution. To confirm this, we defined the area controlled by each river as the area where the dilution ratio is larger than 10%. As shown in Fig. 6, the concentrations of SMX in these areas are almost linearly related to salinity. As previously noted, C is linearly related to S when C_{rn} is constant and a_n equals D_{rn}, with the slope and intercept given as $-\frac{C_{rn}}{S_0}$ and C_{rn}, respectively. As shown in Fig. 6 and Table S4, the regression lines between SMX concentrations and salinity have slopes and intercepts close to the analytical values ($-\frac{C_{rn}}{S_0}$ and C_{rn}) deduced above.

4.2. Simulation of SMX with different half-lives and pollution prediction in the UGoT

As the decomposition of SMX is affected by light, dissolved oxygen, and other environmental variables, its half-life has a large range (Benotti and Brownawell, 2009; Xu et al., 2009; Baumgarten et al., 2011). To investigate how the half-life of SMX affects its behavior in seawater, we altered the half-life in the model and repeated the calculations. As shown in Fig. 3, S3, and S4, half-life had little effect on the seasonal variation and spatial pattern of SMX, although spatially averaged concentrations increased with increasing half-life.

The area of UGoT is small and river inputs are the main sources of SMX in the coastal sea, meaning that spatially averaged concentrations can be predicted based on river input fluxes and SMX half-life. As inferred from Eq. (1), SMX concentrations are linearly related to river input, and its decomposition is represented by the first-order model. Therefore, a prediction function of spatially averaged SMX concentration (C_p) is given as follows:

$$C_p = A \times r_s \times e^{\frac{B}{\alpha}} \tag{9}$$

where r_s and α are the river input (kg day^{-1}) of the pollutant and its half-life (day), respectively; and A and B are constants obtained from the model results. Using seven different SMX half-lives in the model simulations, we obtained 28 sets of data for each month to determine A and B values of approximately 2.1 and −31, respectively (Fig. S5), that remain relatively constant between months. By substituting A and B into Eq. (9), we obtained concentration values corresponding to a range of river input fluxes and half-lives (Fig. 7). While we have focused on SMX, it is important to note that this approach can be applied to any pollutant with a river input flux and half-life within the modeled range. Based on Fig. 7, the concentration of a pollutant will increase with an increase in river input flux and its half-life. Moreover, concentrations increase more rapidly with river input flux for pollutants with a longer half-life (Fig. 7).

The predicted no-effect concentrations (PNECs) of SMX for resistance selection and ecotoxicological effects are 16,000 μg m^{-3} and 590 μg m^{-3}, respectively (Bengtsson-Palme and Larsson, 2016), which are far higher than those reported here. Furthermore, Eq. (9) can be used to

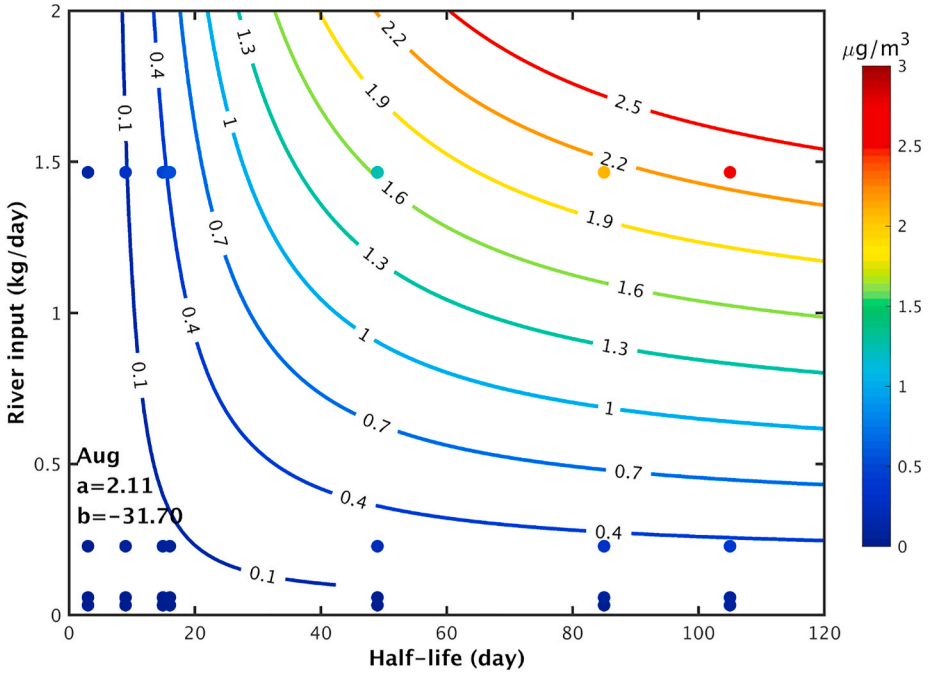

Fig. 7. Predicted concentrations of pollutants in the UGoT in August based on river input flux (kg day^{-1}) and half-life (day). Dots are the model results and lines represent the predicted results.

calculate the critical river input flux of a pollutant where its half-life and PNEC are known. For example, in August, the critical river flux of SMX is 61,099 kg day^{-1} for C_p to remain lower than the PNEC for resistance selection, and 2253 kg day^{-1} for ecotoxicological effects.

We also calculated the flushing time of SMX based on its half-life. As defined in Section 3.3, this is the ratio of SMX mass to the flux associated with its removal. In the model, when the decomposition flux of SMX is much larger than its exchange rate with the open sea through the lateral boundary, the flushing time approaches a ratio dependent on its half-life., thus:

$$t_r = \frac{M}{F_{cwd}} \tag{10}$$

$$M = C_m \times V \tag{11}$$

$$F_{cwd} = \frac{\ln 2}{\alpha} \times C_m \times V \tag{12}$$

where M (kg) is the annual mean of pollutant mass inside the UGoT, F_{cwd} (kg day^{-1}) is the pollution flux from decomposition, C_m (μg m^{-3}) is the annual mean pollution concentration inside the UGoT, V (m^3) is the water volume of the UGoT, and α (day) is the half-life. To deduce the theoretical relationship between flushing time and half-life, Eqs. (11) and (12) assume that SMX concentrations are temporally and spatially homogeneous. From Eqs. (10)–(12), it can be concluded that $t_r = \frac{\alpha}{\ln 2}$ (13). Thus, the flushing time of SMX is linearly related to its half-life.

Figure S7a shows the SMX predicted flushing times with half-life as the dependent variable and this function can be applied to any pollutant with a half-life within the modeled range. It must be noted that the prediction function is based on the condition that decomposition flux is much larger than the exchange rate with the open sea; a value of 8 was selected as the critical ratio of decomposition flux to the exchange rate through the lateral boundary to judge their relative magnitudes. This ratio corresponds to a critical half-life. A full function between these variables is shown in Fig. S7b, the derivation of which is detailed in Appendix D. The critical half-life is calculated as 109 days when the ratio of the decomposition flux to lateral boundary flux is equal to 8. In other words, the function shown in Fig. S7a can be used to predict the flushing time of a pollutant from rivers in the UGoT when its half-life is less than or equal to 109 days.

In Section 3, we presented results assuming a constant river input flux of SMX throughout a year. Here, we introduce an alternative assumption that the SMX concentrations in river waters are constant throughout the year and the detailed results are shown in Appendix E.

5. Conclusions

A 3D physical-antibiotic model was developed to investigate the transport and dilution of SMX from rivers in the UGoT. The simulated concentrations of SMX generally match the field data and vary slightly between seasons despite assuming a constant input flux from the rivers. The horizontal distribution of SMX concentrations varies significantly between months, which is affected by the residual currents associated with the monsoon and river runoff. SMX concentrations also vary vertically in the areas close to estuaries but are vertically homogeneous offshore. The dilution ratios indicate that SMX concentrations become less than 10% of those in river waters over a short distance from the estuaries. The dilution effect does vary between rivers, depending on the locations of their estuaries and the residual currents in the UGoT. Overall, input from the Chaopraya River is the main source (82%) of SMX in the UGoT, the vast majority of which (98%) is naturally decomposed.

A linear relationship between fluvial pollutant concentrations and seawater salinity occurs only when concentrations are equal between the rivers and when the pollutant is quasi-persistent. Therefore, the relationship between SMX concentrations and salinity is not linear in the UGoT. Nevertheless, a linear relationship can be assumed in those areas mainly affected by a single river, which we defined using the 10% dilution ratio. Moreover, we established prediction functions for mean concentrations and flushing times of non-persistent pollutants in the UGoT based on half-lives and river input flux.

The fundamental simulation scheme for the transport of non-persistent organic pollutants in the sea is conducted in this work. It is useful to quantitatively examine the behaviors of pollutants in seawater and predict pollutant concentrations and spatial variations. The biogeochemical cycle of antibiotics in the marine environment is complex including uptake by phytoplankton as well as bacteria, water-suspended particle partitioning, and adsorption onto sediment (Xu et al., 2009; Li, 2014; Bai and Acharya, 2016; Puckowski et al., 2016; Yu et al., 2017). In our model, we partially represented these processes by considering the flux of SMX via decomposition. However, given their significance for estimating the ecological risk and fate of antibiotics in the sea, more effort is now required to incorporate them more fully in future models.

Declaration of competing interest

The authors declare that they have no known competing financial interests or personal relationships that could have appeared to influence the work reported in this paper.

Acknowledgment

This study is funded by the Ministry of Education, Culture, Sports, Science and Technology, Japan (MEXT) to a project on Joint Usage/Research Center–Leading Academia in Marine and Environment Pollution Research (LaMer). This work is also supported by Sasakawa fund of the Japan Science Society (No. 2021–2028).

Appendix A. Supplementary data

Supplementary data to this article can be found online at https://doi.org/10.1016/j.envpol.2021.117779.

Credit author statement

Aobo Wang: Conceptualization; Methodology; Software; Validation; Formal analysis; Data curation; Writing – original draft. **Xinyu Guo**: Conceptualization; Methodology; Validation; Writing – review & editing; Visualization. **Akihiko Morimoto**: Validation; Investigation; Writing – review & editing. **Kana Maetani**: Validation; Investigation. **Rumi Tanoue**: Resources; Writing – review & editing. **Siraporn Tong-U-Dom**: Investigation; Resources. **Anukul Buranapratheprat**: Writing – review & editing.

References

Bai, X., Acharya, K., 2016. Removal of trimethoprim, sulfamethoxazole, and triclosan by the green alga Nannochloris sp. J. Hazard Mater. 315, 70–75. https://doi.org/10.1016/j.jhazmat.2016.04.067.

Baumgarten, B., Jährig, J., Reemtsma, T., Jekel, M., 2011. Long term laboratory column experiments to simulate bank filtration: factors controlling removal of sulfamethoxazole. Water Res. 45, 211–220. https://doi.org/10.1016/j.watres.2010.08.034.

Bengtsson-Palme, J., Larsson, D.G.J., 2016. Concentrations of antibiotics predicted to select for resistant bacteria: proposed limits for environmental regulation. Environ. Int. 86, 140–149. https://doi.org/10.1016/j.envint.2015.10.015.

Benotti, M.J., Brownawell, B.J., 2009. Microbial degradation of pharmaceuticals in estuarine and coastal seawater. Environ. Pollut. 157, 994–1002. https://doi.org/10.1016/j.envpol.2008.10.009.

Bian, C., Jiang, W., Greatbatch, R.J., 2013. An exploratory model study of sediment transport sources and deposits in the Bohai Sea, Yellow Sea, and East China Sea. J. Geophys. Res. Ocean. 118, 5908–5923. https://doi.org/10.1002/2013JC009116.

Björlenius, B., Ripszám, M., Haglund, P., Lindberg, R.H., Tysklind, M., Fick, J., 2018. Pharmaceutical residues are widespread in Baltic Sea coastal and offshore waters –

screening for pharmaceuticals and modelling of environmental concentrations of carbamazepine. Sci. Total Environ. 633, 1496–1509. https://doi.org/10.1016/j.scitotenv.2018.03.276.
Bonvin, F., Omlin, J., Rutler, R., Schweizer, W.B., Alaimo, P.J., Strathmann, T.J., McNeill, K., Kohn, T., 2013. Direct photolysis of human metabolites of the antibiotic sulfamethoxazole: evidence for abiotic back-transformation. Environ. Sci. Technol. 47, 6746–6755. https://doi.org/10.1021/es303777k.
Boonyatumanond, R., Wattayakorn, G., Amano, A., Inouchi, Y., Takada, H., 2007. Reconstruction of pollution history of organic contaminants in the upper Gulf of Thailand by using sediment cores: first report from Tropical Asia Core (TACO) project. Mar. Pollut. Bull. 54, 554–565. https://doi.org/10.1016/j.marpolbul.2006.12.007.
Buranapratheprat, A., Yanagi, T., Olaf Niemann, K., Matsumura, S., Sojisuporn, P., 2008. Surface chlorophyll-a dynamics in the upper Gulf of Thailand revealed by a coupled hydrodynamic-ecosystem model. J. Oceanogr. 64, 639–656. https://doi.org/10.1007/s10872-008-0054-9.
Burnett, W.C., Wattayakorn, G., Taniguchi, M., Dulaiova, H., Sojisuporn, P., Rungsupa, S., Ishitobi, T., 2007. Groundwater-derived nutrient inputs to the upper Gulf of Thailand. Continent. Shelf Res. 27, 176–190. https://doi.org/10.1016/j.csr.2006.09.006.
Chen, H., Jing, L., Teng, Y., Wang, J., 2018. Characterization of antibiotics in a large-scale river system of China: occurrence pattern, spatiotemporal distribution and environmental risks. Sci. Total Environ. 618, 409–418. https://doi.org/10.1016/j.scitotenv.2017.11.054.
Downs, C.A., Kramarsky-Winter, E., Segal, R., Fauth, J., Knutson, S., Bronstein, O., Ciner, F.R., Jeger, R., Lichtenfeld, Y., Woodley, C.M., Pennington, P., Cadenas, K., Kushmaro, A., Loya, Y., 2016. Toxicopathological effects of the sunscreen UV filter, oxybenzone (Benzophenone-3), on coral planulae and cultured primary cells and its environmental contamination in Hawaii and the U.S. Virgin islands. Arch. Environ. Contam. Toxicol. 70, 265–288. https://doi.org/10.1007/s00244-015-0227-7.
Drillia, P., Dokianakis, S.N., Fountoulakis, M.S., Kornaros, M., Stamatelatou, K., Lyberatos, G., 2005. On the occasional biodegradation of pharmaceuticals in the activated sludge process: the example of the antibiotic sulfamethoxazole. J. Hazard Mater. 122, 259–265. https://doi.org/10.1016/j.jhazmat.2005.03.009.
Du, J., Zhao, H., Liu, S., Xie, H., Wang, Y., Chen, J., 2017. Antibiotics in the coastal water of the South Yellow Sea in China: occurrence, distribution and ecological risks. Sci. Total Environ. 595, 521–527. https://doi.org/10.1016/j.scitotenv.2017.03.281.
Isidori, M., Lavorgna, M., Nardelli, A., Pascarella, L., Parrella, A., 2005. Toxic and genotoxic evaluation of six antibiotics on non-target organisms. Sci. Total Environ. 346, 87–98. https://doi.org/10.1016/j.scitotenv.2004.11.017.
Jia, A., Hu, J., Wu, X., Peng, H., Wu, S., Dong, Z., 2011. Occurrence and source apportionment of sulfonamides and their metabolites in Liaodong Bay and the adjacent Liao River basin, North China. Environ. Toxicol. Chem. 30, 1252–1260. https://doi.org/10.1002/etc.508.
Jiang, L., Hu, X., Yin, D., Zhang, H., Yu, Z., 2011. Occurrence, distribution and seasonal variation of antibiotics in the Huangpu River, Shanghai, China. Chemosphere 82, 822–828. https://doi.org/10.1016/j.chemosphere.2010.11.028.
Ju, T., Ge, W., Jiang, T., Chai, C., 2016. Polybrominated diphenyl ethers in dissolvedand suspended phases of seawater and in surface sediment from Jiaozhou Bay, North China. Sci. Total Environ. 557–558, 571–578. https://doi.org/10.1016/j.scitotenv.2016.03.013.
Kafaei, R., Papari, F., Seyedabadi, M., Sahebi, S., Tahmasebi, R., Ahmadi, M., Sorial, G. A., Asgari, G., Ramavandi, B., 2018. Occurrence, distribution, and potential sources of antibiotics pollution in the water-sediment of the northern coastline of the Persian Gulf, Iran. Sci. Total Environ. 627, 703–712. https://doi.org/10.1016/j.scitotenv.2018.01.305.
Ko, F.C., Chang, C.W., Cheng, J.O., 2014. Comparative study of polycyclic aromatic hydrocarbons in coral tissues and the ambient sediments from Kenting National Park, Taiwan. Environ. Pollut. 185, 35–43. https://doi.org/10.1016/j.envpol.2013.10.025.
Kümmerer, K., 2009. Antibiotics in the aquatic environment - a review - Part I. Chemosphere 75, 417–434. https://doi.org/10.1016/j.chemosphere.2008.11.086.
Li, S., Shi, W., Liu, W., Li, H., Zhang, W., Hu, J., Ke, Y., Sun, W., Ni, J., 2018. A duodecennial national synthesis of antibiotics in China's major rivers and seas (2005–2016). Sci. Total Environ. 615, 906–917. https://doi.org/10.1016/j.scitotenv.2017.09.328.
Li, W.C., 2014. Occurrence, sources, and fate of pharmaceuticals in aquatic environment and soil. Environ. Pollut. 187, 193–201. https://doi.org/10.1016/j.envpol.2014.01.015.
Li, X., Hai, F.I., Nghiem, L.D., 2011. Simultaneous activated carbon adsorption within a membrane bioreactor for an enhanced micropollutant removal. Bioresour. Technol. 102, 5319–5324. https://doi.org/10.1016/j.biortech.2010.11.070.
Martínez, J.L., 2008. Antibiotics and antibiotic resistance genes in natural environments. Science (80- 321, 365–367. https://doi.org/10.1126/science.1159483.
Mellor, G.L., Häkkinen, S.M., Ezer, T., Patchen, R.C., 2002. A generalization of a sigma coordinate ocean model and an intercomparison of model vertical grids. In: Pinardi, N., Woods, J. (Eds.), Ocean Forecasting: Conceptual Basis and Applications. Springer, Berlin, pp. 55–72. https://doi.org/10.1007/978-3-662-22648-3_4.
Monsen, N.E., Cloern, J.E., Lucas, L.V., Monismith, S.G., 2002. A comment on the use of flushing time, residence time, and age as transport time scales. Limnol. Oceanogr. 47, 1545–1553. https://doi.org/10.4319/lo.2002.47.5.1545.
Mrozik, W., Vinitnantharat, S., Thongsamer, T., Pansuk, N., Pattanachan, P., Thayanukul, P., Acharya, K., Baluja, M.Q., Hazlerigg, C., Robson, A.F., Davenport, R. J., Werner, D., 2019. The food-water quality nexus in periurban aquacultures downstream of Bangkok, Thailand. Sci. Total Environ. 695, 133923. https://doi.org/10.1016/j.scitotenv.2019.133923.
Nödler, K., Licha, T., Barbieri, M., Pérez, S., 2012. Evidence for the microbially mediated abiotic formation of reversible and non-reversible sulfamethoxazole transformation products during denitrification. Water Res. 46, 2131–2139. https://doi.org/10.1016/j.watres.2012.01.028.
Puckowski, A., Mioduszewska, K., Łukaszewicz, P., Borecka, M., Caban, M., Maszkowska, J., Stepnowski, P., 2016. Bioaccumulation and analytics of pharmaceutical residues in the environment: a review. J. Pharmaceut. Biomed. Anal. 127, 232–255. https://doi.org/10.1016/j.jpba.2016.02.049.
Sabourin, D.T., Silliman, J.E., Strychar, K.B., 2012. Polycyclic aromatic hydrocarbon contents of coral and surface sediments off the south Texas coast of the Gulf of Mexico. Int. J. Biol. 5, 1–12. https://doi.org/10.5539/ijb.v5n1p1.
Tamtam, F., Mercier, F., Le Bot, B., Eurin, J., Tuc Dinh, Q., Clément, M., Chevreuil, M., 2008. Occurrence and fate of antibiotics in the Seine River in various hydrological conditions. Sci. Total Environ. 393, 84–95. https://doi.org/10.1016/j.scitotenv.2007.12.009.
Tewari, S., Jindal, R., Kho, Y.L., Eo, S., Choi, K., 2013. Major pharmaceutical residues in wastewater treatment plants and receiving waters in Bangkok, Thailand, and associated ecological risks. Chemosphere 91, 697–704. https://doi.org/10.1016/j.chemosphere.2012.12.042.
Wang, A., Guo, X., Shi, J., Luo, C., Gao, H., 2019a. A simulation of the seasonal variation of decabromodiphenyl ether in a bay adjacent to the Yellow Sea. Sci. Total Environ. 664, 522–535. https://doi.org/10.1016/j.scitotenv.2019.01.385.
Wang, Y., Guo, X., Zhao, L., Zhang, J., 2019b. Seasonal variations in nutrients and biogenic particles in the upper and lower layers of East China Sea Shelf and their export to adjacent seas. Prog. Oceanogr. 176, 102138. https://doi.org/10.1016/j.pocean.2019.102138.
Watkinson, A.J., Murby, E.J., Kolpin, D.W., Costanzo, S.D., 2009. The occurrence of antibiotics in an urban watershed: From wastewater to drinking water. Sci. Total Environ. 407 (8), 2711–2723. https://doi.org/10.1016/j.scitotenv.2008.11.059.
Xu, B., Mao, D., Luo, Y., Xu, L., 2011. Sulfamethoxazole biodegradation and biotransformation in the water-sediment system of a natural river. Bioresour. Technol. 102, 7069–7076. https://doi.org/10.1016/j.biortech.2011.04.086.
Xu, W.H., Zhang, G., Wai, O.W.H., Zou, S.C., Li, X.D., 2009. Transport and adsorption of antibiotics by marine sediments in a dynamic environment. J. Soils Sediments 9, 364–373. https://doi.org/10.1007/s11368-009-0091-z.
Yu, X., Guo, X., Morimoto, A., Buranapratheprat, A., 2018. Simulation of river plume behaviors in a tropical region: case study of the Upper Gulf of Thailand. Continent. Shelf Res. 153, 16–29. https://doi.org/10.1016/j.csr.2017.12.007.
Yu, Y., Zhou, Y., Wang, Z., Torres, O.L., Guo, R., Chen, J., 2017. Investigation of the removal mechanism of antibiotic ceftazidime by green algae and subsequent microbic impact assessment. Sci. Rep. 7, 1–11. https://doi.org/10.1038/s41598-017-04128-3.
Zhang, J., Guo, X., Zhao, L., 2019. Tracing external sources of nutrients in the East China Sea and evaluating their contributions to primary production. Prog. Oceanogr. 176, 102122. https://doi.org/10.1016/j.pocean.2019.102122.
Zhang, Q.Q., Ying, G.G., Pan, C.G., Liu, Y.S., Zhao, J.L., 2015. Comprehensive evaluation of antibiotics emission and fate in the river basins of China: source analysis, multimedia modeling, and linkage to bacterial resistance. Environ. Sci. Technol. 49, 6772–6782. https://doi.org/10.1021/acs.est.5b00729.
Zhang, R., Tang, J., Li, J., Cheng, Z., Chaemfa, C., Liu, D., Zheng, Q., Song, M., Luo, C., Zhang, G., 2013a. Occurrence and risks of antibiotics in the coastal aquatic environment of the Yellow Sea, North China. Sci. Total Environ. 450–451, 197–204. https://doi.org/10.1016/j.scitotenv.2013.02.024.
Zhang, R., Tang, J., Li, J., Zheng, Q., Liu, D., Chen, Y., Zou, Y., Chen, X., Luo, C., Zhang, G., 2013b. Antibiotics in the offshore waters of the Bohai Sea and the Yellow Sea in China: occurrence, distribution and ecological risks. Environ. Pollut. 174, 71–77. https://doi.org/10.1016/j.envpol.2012.11.008.
Zhang, Ruijie, Zhang, Ruiling, Yu, K., Wang, Y., Huang, X., Pei, J., Wei, C., Pan, Z., Qin, Z., Zhang, G., 2018. Occurrence, sources and transport of antibiotics in the surface water of coral reef regions in the South China Sea: potential risk to coral growth. Environ. Pollut. 232, 450–457. https://doi.org/10.1016/j.envpol.2017.09.064.
Zhu, J., Guo, X., Shi, J., Gao, H., 2019. Dilution characteristics of riverine input contaminants in the Seto Inland Sea. Mar. Pollut. Bull. 141, 91–103. https://doi.org/10.1016/j.marpolbul.2019.02.029.
Zou, S., Xu, W., Zhang, R., Tang, J., Chen, Y., Zhang, G., 2011. Occurrence and distribution of antibiotics in coastal water of the Bohai Bay, China: impacts of river discharge and aquaculture activities. Environ. Pollut. 159, 2913–2920. https://doi.org/10.1016/j.envpol.2011.04.037.
Zuccato, E., Castiglioni, S., Bagnati, R., Melis, M., Fanelli, R., 2010. Source, occurrence and fate of antibiotics in the Italian aquatic environment. J. Hazard Mater. 179, 1042–1048. https://doi.org/10.1016/j.jhazmat.2010.03.110.